Journal of Marine Systems 83 (2010) 242–252

Contents lists available at ScienceDirect

Journal of Marine Systems

journal homepage: www.elsevier.com/locate/jmarsys

Application of a 3D Lagrangian model to explain the decline of a *Dinophysis acuminata* bloom in the Bay of Biscay

L. Velo-Suárez [a,*], B. Reguera [a], S. González-Gil [b], M. Lunven [c], P. Lazure [c], E. Nézan [d], P. Gentien [c,1]

[a] Instituto Español de Oceanografía, Centro Oceanográfico de Vigo, Aptdo. 1552, E-36200 Vigo, Spain
[b] Instituto Español de Oceanografía, Centro Oceanográfico de Madrid, Orense 58, 7ª planta, E-28020 Madrid, Spain
[c] IFREMER, Centre de Brest. DYNECO. Pointe du Diable BP70, E-29280 Plouzané, France
[d] IFREMER, 13, rue de Kérose, Le Roudouic E-29187 Concarneau Cedex, France

ARTICLE INFO

Article history:
Received 15 September 2009
Received in revised form 18 May 2010
Accepted 21 May 2010
Available online 2 June 2010

Keywords:
Lagrangian individual particle-tracking models
Harmful algal blooms
Dinophysis acuminata
Physical–biological interactions
Bay of Biscay

ABSTRACT

During July 2006, a cruise was carried out in the Northern Bay of Biscay (off Brittany, France) to study meso- and microscale patterns of phytoplankton distribution. Moderate concentrations (10^2–10^3 cells L^{-1}) of *Dinophysis acuminata* were constrained to specific depths (upper layers above the pycnocline) at stations with lower surface salinity (34.5) and steep temperature gradients (18–13.5 °C between 4 and 7 m depth) within the Loire and Vilaine river plumes. On board incubations revealed a healthy *D. acuminata* population at the biomass maxima with 89% of viable (FDA-treated) cells and moderate division rates (up to 0.10 d^{-1}). Despite its good physiological condition, the population of *D. acuminata* declined rapidly to undetectable levels during the second leg of the cruise.

A 3D Lagrangian Particle-Tracking Model (3D LPTM) was used to simulate the transport of *D. acuminata* cells in the Loire and Vilaine river plumes from 15 June to 30 July. This 3D LPTM model was coupled to a MARS3D (Model for Applications at Regional Scale) model previously calibrated and validated for the region. Model results suggest that physical processes alone could explain the dispersion of the *D. acuminata* population within the area. The application of a 3D-LPTM model shows how individual based model approaches are valuable to identify *Dinophysis* spp. transport pathways and reproduce retention/dispersion patterns observed in the field.

1. Introduction

Seasonal blooms of *Dinophysis acuminata* associated with DSP (Diarrheic Shellfish Poisoning) outbreaks have been nearly annual features in different regions of the Northern Bay of Biscay, especially the Bay of Vilaine (BV) and south Brittany (Delmas et al., 1992; Xie et al., 2007).

Changes in *D. acuminata* concentrations result from the balance between gains (growth and physical accumulation) and losses (grazing, mortality and physical dispersion). Knowledge of the variations of these parameters is thus fundamental to understanding the processes leading to *Dinophysis* bloom dynamics. Although some attempts have been made to understand *D. acuminata* population dynamics in this area (Xie et al., 2007), little is known about the processes that trigger the decline of *D. acuminata* populations. In contrast, physical factors (temperature and salinity gradients; transport) have been identified as key controls of the initiation and distribution of *Dinophysis* blooms at a regional scale. Delmas et al. (1993) suggested that *D. acuminata* blooms originate offshore and are later transported to coastal areas of the BV by currents. This hypothesis was tested by Xie et al. (2007) who used a 3D model to explore the role of offshore retention areas and their subsequent advection to the coast in promoting coastal DSP outbreaks. These authors concluded that small-scale eddies and their inshore advection were related to the beginning of the *Dinophysis* spp. season in the BV. Other studies in the region have shown that *D. acuminata* populations are mainly concentrated around marked temperature and salinity gradients in the water column (Gentien et al., 1995; Maestrini, 1998; Marcaillou et al., 2001; Lunven et al., 2005). Density gradients have been proposed to affect bloom development (Maestrini, 1998), but their real impact in the field remains poorly understood. Horizontal confinement of *D. acuminata* blooms in the Loire and Vilaine river plumes has also been reported by Marcaillou et al. (2001).

Understanding of *D. acuminata* dynamics requires an integrated strategy that includes not only observations but also modelling. Models can help to identify the key processes in *D. acuminata* population dynamics and they are essential tools to understand its complexity. A thorough understanding of the physiological status of the population and of the bloom's intensity, geographical extent, duration, and decline is needed for the ultimate prediction of HAB dynamics.

* Corresponding author. Instituto Español de Oceanografía, Centro Oceanográfico de Vigo, Aptdo, 1552, E-36200 Vigo, Spain. Tel.: +34 986 492111; fax: +34 986 498626.
E-mail address: lourdesvelo@gmail.es (L. Velo-Suárez).
[1] Deceased.

0924-7963/$ – see front matter © 2010 Elsevier B.V. All rights reserved.
doi:10.1016/j.jmarsys.2010.05.011

3D Lagrangian particle-tracking models (3D LPTMs) and individual based models (IBM) have been used by oceanographers during the past two decades to explore processes that influence the transport of eggs and developing larval stages of invertebrates and fish (Gallego et al., 2007). 3D-LPTM models can provide new insights into physical–biological interactions that affect plankton dispersal, growth and survival and enhance our understanding of plankton population variability and structure (North et al., 2009). Previous studies have shown how the application of this kind of models has helped to explain the transport/retention of fish larvae in Iberian shelf waters (Santos et al., 2007).

During summer 2006, a three-week multidisciplinary cruise was conducted to describe the fine-scale physical and biological structure of the water column and to study meso- and microscale patterns of phytoplankton distribution in the Northern Bay of Biscay. Simulations from a 3D LPTM (Ichthyop; Lett et al., 2008) were used to analyze the influence of physical transport on the distribution of a *D. acuminata* population during late stages of the bloom from mid June to the end of July 2006. This work represents the first application of a 3D LPTM model to study the decline of a harmful dinoflagellate (*D. acuminata*) bloom located in the Loire and Vilaine river plumes, off Brittany (Bay of Biscay).

2. Material and methods

2.1. The study area

The northern Bay of Biscay is located in the northeastern Atlantic off the Brittany coasts (France) (Fig. 1). This part of the Bay receives fresh water from the Loire and Vilaine rivers whose watershed areas (128 800 km^2) account for 95% of the total catchment area of the northern Bay of Biscay. Haline stratification is strong from February to June in response to high river runoff and relatively low vertical mixing; thermal stratification occurs between May and mid-September in a ~50 m thick layer, whereas the water column remains thermally homogenous from January to the beginning of April (Lazure and Jegou, 1998). Winds show an annual cycle whose main characteristic is the spring (late March) shift from southwesterly to west-northwesterly winds (Lazure et al., 2008).

2.2. REPHY data

Concentrations of *D. acuminata* throughout the year were obtained from the French HAB monitoring programme (REPHY, IFREMER) database (http://www.ifremer.fr/envlit/surveillance/rephy.htm). Hydrobios bottle samples (5 m depth) were collected biweekly at 7 different stations in the BV. In this programme, phytoplankton quantitative analyses are carried out according to the Utermöhl (1931) method. Samples are counted after sedimentation (4 h minimum) of 10 mL columns under an inverted light microscope (IX70 Olympus) fitted with 100×, 200× and 400× objectives and phase-contrast optics. Early warning on the presence of harmful species was obtained from the observation of phytoplankton net-haul samples.

2.3. Cruise sampling overview

Studies were carried out on board *R/V Thalassa* from 6 to 22 July 2006. Sampling stations from the first (6–12 July) and second (13–22 July) legs of the cruise are shown in Fig. 2 and Table 1. To obtain qualitative information on phytoplankton distribution, vertical plankton net (20-µm mesh; 20 m depth) hauls were collected at each station. Plankton net samples were examined immediately on board under a Nikon ECLIPSE TE2000-S inverted microscope at 100× and 400× magnification.

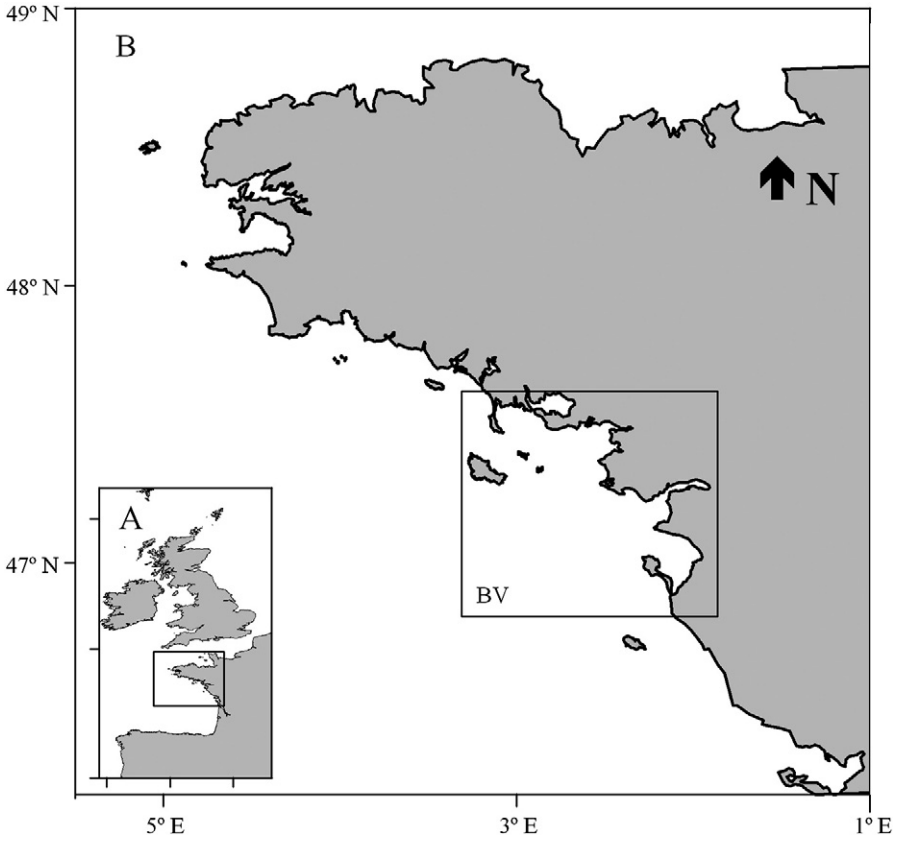

Fig. 1. (A) Map of Western Europe and location of the Northern Bay of Biscay. (B) Location of the Bay of Vilaine (BV) in the Northern Bay of Biscay.

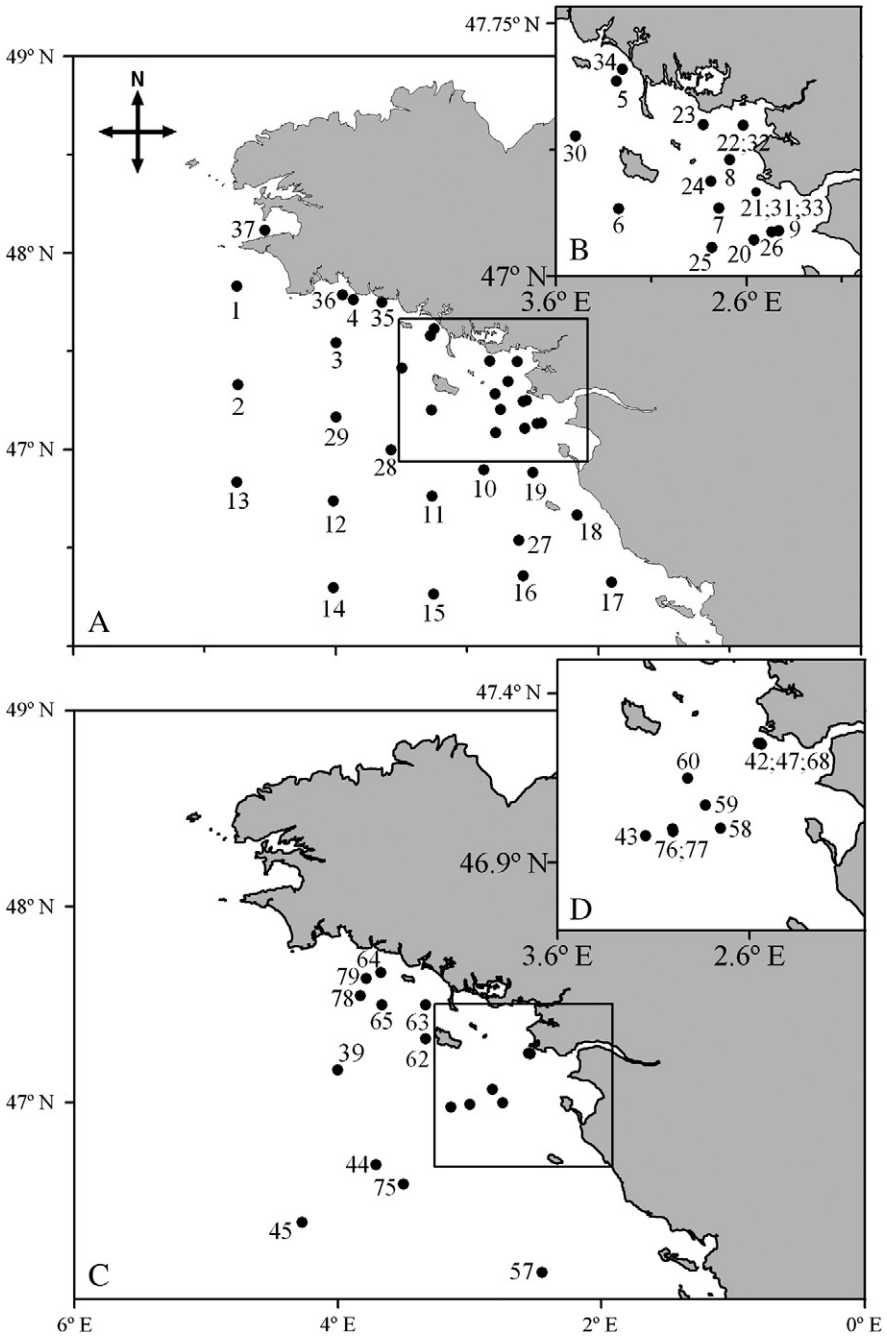

Fig. 2. Spatial distribution of sampling sites in the Northern Bay of Biscay during the first (A, B) and the second legs (C, D) of the survey.

Table 1
Temporal distribution of sampling sites in the Northern Bay of Biscay during the first and the second legs of the survey.

Leg 1		Leg 2	
Date (July)	Sampling stations	Date (July)	Sampling stations
06	1–4	13	38
07	5–10	14	39–41
08	11–15	15	42–45
09	16–21	16	47
10	22–28	18	57–63
11	29–33	19	64–68
12	34–37	20	71
		21	75,77
		22	78–79

Measurements in the water column were carried out with the high-resolution IFREMER particle size analyzer profiler (IPSAP), capable of simultaneous resolution of physical and optical structures at small scale (see Gentien et al., 1995; Velo-Suárez et al., 2008 for details). The IPSAP profiler includes a fluorescence sensor (Seapoint Sensors, Inc., Exeter, New Hampshire, USA) attached to a SBE25 CTD probe (Sea-Bird Electronics, Washington, USA) coupled to an *in situ* particle size analyzer (Gentien et al., 1995). The latter is needed as guidance for sampling, since it detects specific particle profiles, helping to distinguish between layers with abundant organic aggregates and those with dinoflagellates in the 36–64 µm size fraction. The SBE25 probe allows real time data acquisition of standard parameters, such as depth, temperature, salinity, chlorophyll-like *in vivo* fluorescence and photosynthetically active radiation (PAR). The CTD fluorometer was calibrated with laboratory cultures of the

diatom *Chaetoceros gracile* using the trichromatic method for chlorophyll determination according to Aminot and Kerouel (2004). IPSAP data were post-processed to obtain average values every 50-cm.

A rosette (12 5-L Niskin bottles) attached to the IPSAP profiler was used to sample at the exact depth of the sensors. At each station, the IPSAP profiler was lowered at a speed of 0.3 ms^{-1}, allowing an accurate assessment of the hydrological characteristics of the water column and the detection of water layers with distinct characteristics. During the up-cast, the instrument was stopped and two Niskin bottles were closed at the depths where structures of interest (fluorescence and particle load maxima, pycnocline, and other density discontinuities) were detected. After retrieval of the profiler, water samples from each bottle were immediately well mixed and aliquots taken for biological analysis.

From each depth, a 2 L sample was gently concentrated through a 20 µm mesh and the filtered material resuspended in a volume of approximately 20 mL; 3 mL of this concentrate were poured into a sedimentation slide for *in vivo* observations and for a quick rough estimate of *Dinophysis* abundance. For quantitative analyses of microphytoplankton, two kinds of samples were taken: (1) unconcentrated and (2) 2 L seawater samples concentrated through 20 µm filters, that were further resuspended in a final volume of 30 mL (factor = 66.6). Samples were preserved in acidic Lugol's solution and analyzed under an inverted microscope (Nikon ECLIPSE TE2000-S) according to the Utermöhl (1931) method. Phytoplankton abundance was determined to species level when possible. Concentrations of smaller and more abundant species were estimated from two transects counted at 400× magnification (detection limit: 40 cells L^{-1}) after sedimentation of 25 mL aliquots of the unconcentrated samples. In the case of less abundant species (including *Dinophysis* spp.), specimens from the whole chamber were enumerated at a magnification of 100× after sedimentation of 3 mL aliquots of the concentrated samples. In the last case, the detection limit in cell counts was 5 cells L^{-1}.

2.4. D. acuminata in vivo observations and incubation experiments

On board observations of the physiological status of *D. acuminata* from live samples were performed under a Nikon ECLIPSE TE2000-S inverted microscope (Nikon Instruments Europe B.V., The Netherlands) with Differential Interference Contrast (DIC) and epifluorescence under a blue filter set (excitation 450–490 nm, emission 520 nm LP). Snapshots were taken with a Nikon D70 camera coupled to the microscope at magnifications of 100× and 400×. Observations included annotations on chlorophyll (red) and phycoerythrin (orange) autofluorescence in *D. acuminata* and detection and frequency of cells parasitized by *Amoebophrya* spp., which exhibited a characteristic green autofluorescence.

Viability assays of *D. acuminata* cells were carried out with specimens stained with fluorescein diacetate (FDA; Sigma Chemicals, St. Louis, MO, USA). Previous studies with different vital/mortal stains (i.e. SYTOX-Green, Trypan Blue, Calcein-AM) had shown FDA to give the best results with natural populations of *D. acuminata* (Gónzalez-Gil, pers. commun.).

The FDA stock solution of 5 mg mL^{-1} was dissolved in dimethyl sulfoxide (DMSO) and stored at −20 °C. Viability tests were made on samples where *D. acuminata* concentration was higher than 100 cells L^{-1} (Table 2). A portion of the previously concentrated live sample (ca. 3 mL) was transferred to a sedimentation chamber and stained with 5–10 µL of the FDA working solution (5 µM final concentration) and incubated in the dark for 15 min. Viable cells showed green fluorescence after excitation with blue light. Red fluorescence was not considered as an indication of viability since chlorophyll *a* in dead cells may autofluoresce after cell death (Gentien, 1986). Percentages of positive and negative binding were estimated after scanning of at least 100 cells of *D. acuminata* whenever possible.

Table 2
Depth of *D. acuminata* cell maxima at each station where its concentration in the whole water column reached 100 cells L^{-1} during the first leg of the cruise (06–12 July).

Station	Day	Sampling hour (GMT)	*D. acuminata* cells L^{-1}	Depth (m)
8	07 July	12:30	304	7
9	07 July	15:30	148	1.7
20	09 July	21:00	933	4
21	09 July	23:30	707	4
23	10 July	04:00	603	16
26	10 July	01:00	487	1
31	11 July	12:30	1002	2.25
37	12 July	12:00	632	2

For the incubation experiments, 5 L of seawater was concentrated by reverse filtration (Dodson and Thomas, 1978) through a 20 µm mesh to a final volume of about 250 mL. They were maintained in the incubation chamber on board—at 15 ± 1 °C with a 16:8 light: dark photoperiod—in glass cylinders coated with aluminium foil, except the last few centimeters near the top, to enhance accumulation of healthy swimming dinoflagellates in the upper illuminated portion as described in Maestrini et al. (1995). *D. acuminata* cells concentrated in the upper portion of the cylinders were siphoned out and individually picked with microcapillary pipettes under 25× and 100× microscope magnification. Each cell was transferred two to three times to slides with filtered-sterilized seawater (0.2 µm Millipore filters, Millipore Corp. Bedford, MA) and finally placed (individual cells and groups of 5 cells) in culture-plate wells of 0.2 mL containing 150 µL of filtered seawater (FSW) from the same depth of collection. Incubations were examined daily to record the number of cells on each well.

Estimates of division rates (μ) were obtained according to:

$$\mu = \frac{\mathrm{Ln}N_f - \mathrm{Ln}N_0}{t} \quad (1)$$

where μ (d^{-1}) is the specific division rate, N_f and N_0 are the final and initial cell numbers (cell/well) and t is time (d).

2.5. The model

The MARS3D hydrodynamical model (Lazure and Dumas, 2008) for the Northern Bay of Biscay was used to simulate the hydrodynamics in the study area. Model simulations extended from the French coast to 8°W and from the northern Spanish coast to Southern England. The horizontal mesh size used had a resolution of 4 km, and 30 vertical levels were considered with a finer resolution near the surface. The simulation was forced by real conditions of tide, river runoff, heat fluxes and wind using data from the Arpège model of the French Met Office. The model was spun up for 1 year (2005) prior to simulation of the observation period. The model reproduced the main

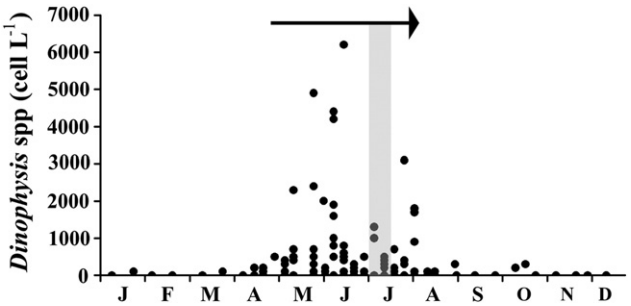

Fig. 3. Weekly distribution of *Dinophysis* spp. during 2006 in the BV (data from REPHY). The extension of the *Dinophysis* season is highlighted with an arrow and the period when cruise sampling was carried out is marked as a shadowed area.

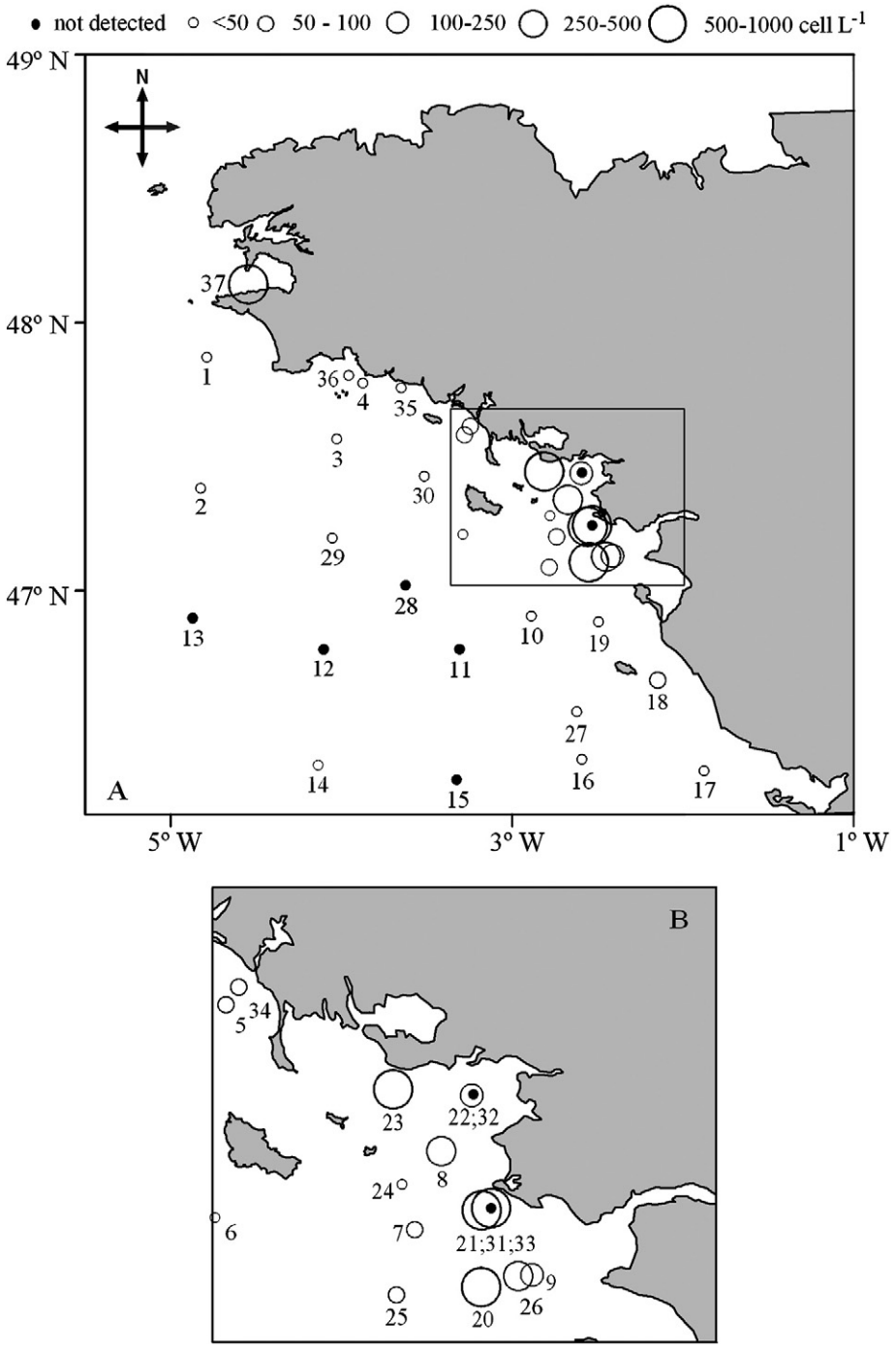

Fig. 4. (A) Horizontal distribution of *D. acuminata* cell maxima in the Northern Bay of Biscay during the first leg of the survey (6–12 July 2006). (B) Detail of the *D. acuminata* horizontal abundance in the BV (6–12 July 2006).

structures detected by remote sensing and *in situ* measurements of the BV during the study time-window.

A Lagrangian individual particle-tracking 3D-model—Ichthyop (Lett et al., 2008)—was used to simulate advection and dispersion of virtual *Dinophysis* populations in the study area. Environmental conditions (3D field of currents, temperature and salinity) between 15 June and 30 July were provided by archived simulations of MARS3D configured for the northern Bay of Biscay. In the BV, two areas were defined: Area 1, which extended from 47.8°N to 47.2°N and from 2.8°W to 2.1°W and roughly corresponds to station 31 from the first leg of the cruise (Fig. 2); and Area 2, which represented the entire BV (Fig. 1), from 46.7°N to 47.8°N and from 2°W to 3.3°W. To test the effect of physical factors on cells transport, the cell movement was defined as that of passive particles.

Two sets of simulations were carried out. In the first set, each simulation consisted of a release of 5000 particles homogeneously distributed within Area 1 every 5 days from 15 June to 30 July (0–20 m depth). Each simulation lasted 10 days. The proportion of particles retained was estimated every 2 m depth from the surface (0 m) to 20 m. Retention was estimated for Areas 1 and 2, and particles that moved out of Area 2 were disregarded.

In the second set, Ichthyop simulations were used to evaluate the trajectory and the retention–dispersion pattern of 1000 virtual particles from 9 to19 July. Particles were uniformly released in Area 1 between 2 and 5 m, i.e. the depth range where *D. acuminata* concentration was highest during the first leg of the survey (see Section 3.5). As in the first set of simulations, particles leaving Area 2 were considered to be lost.

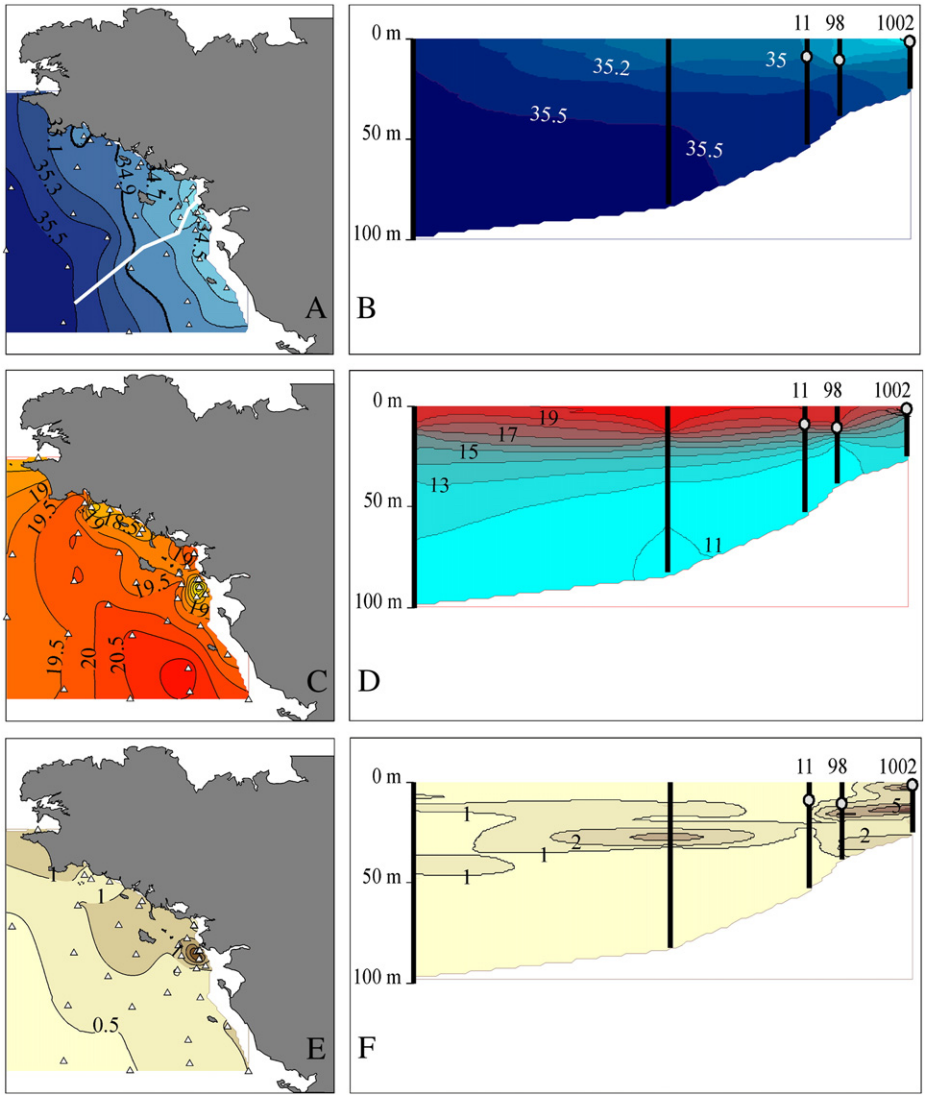

Fig. 5. Surface horizontal distribution of (A) salinity, (C) temperature and (E) particle load measured with the IPSAP profiler in the study area from 6 to 12 July. Triangles in A, C and E indicate sampling points during the first leg. Vertical distribution of (B) salinity, (D) temperature and (F) particle load along a transect off the Loire estuary (shown as a line in panel A). *D. acuminata* maxima (cells L^{-1}) and their location in the water column are also marked in panels B, D, and F.

To achieve realistic simulations, the number of particles released was chosen to be proportional to the maximum concentrations of *D. acuminata* observed on June and July 2006 for the first and second sets of simulations respectively. A sensitivity analysis was carried out to determine whether or not enough particles were being used in each Ichthyop set of simulations. A number of ensemble simulations with different number of particles (100, 500, 1000, 2000 and 5000) were performed. Each ensemble simulation was repeated 30 times to avoid the possible effect of randomness in the particle release process. The analysis of variance (ANOVA) was used to evaluate the statistical differences among ensemble simulations and determine the optimal number of particles to release. ANOVA results showed that there were not significant differences ($p<0.05$) in retention given by the different ensemble simulations. Therefore, the output of Ichthyop using 5000 and 1000 particles was representative of the sets of simulation statistics.

3. Results

3.1. Seasonal distribution of Dinophysis during 2006

The seasonal occurrence of *Dinophysis* spp. in the BV in 2006 showed a rather wide temporal distribution. The *Dinophysis* growth season started by the end of April (Fig. 3) and 2 weeks later, on 15 May 2006, *Dinophysis* populations reached 2300 cells L^{-1}. The highest cell densities (6200 cells L^{-1}) were recorded on 19 June 2006, but at the end of June, *D. acuminata* concentrations declined sharply below 1000 cells L^{-1}. After that, only isolated peaks in *D. acuminata* abundance were detected on 10 July (1200 cells L^{-1}), 31 July (3100 cells L^{-1}), and 07 August (1800 cells L^{-1}). The cruise sampling (6–22 July) was carried out 2 weeks after the seasonal maximum, when *Dinophysis* numbers were decreasing. At the beginning of September 2006, *D. acuminata* was no longer present in significant numbers in the BV.

3.2. Dinophysis spp. distribution during the cruise

During the first leg of the cruise (6–12 July), offshore concentrations of *Dinophysis* spp. were extremely low (<50 cells L^{-1}) but higher values (up to 500 cells L^{-1}) were found in the River Loire and Vilaine plumes at stations with a high particle load, lower surface salinity and steep vertical gradients of temperature (Figs. 4 and 5). Sea surface temperature (SST) estimated from satellite images on 12 July revealed a positive anomaly of 2.98 °C relative to a 22-year (1986–2008) time series (courtesy of Nausicaa, IFREMER). Temperature values obtained

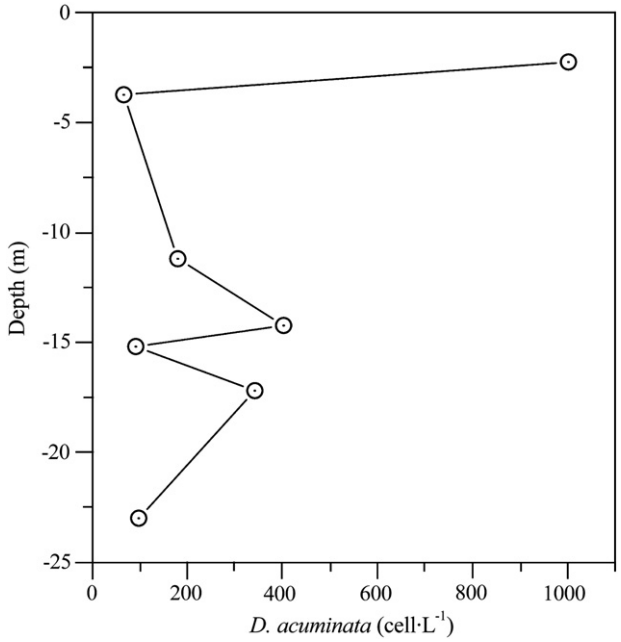

Fig. 6. Vertical distribution of *D. acuminata* at station 31 (BV) on 11 July 2006.

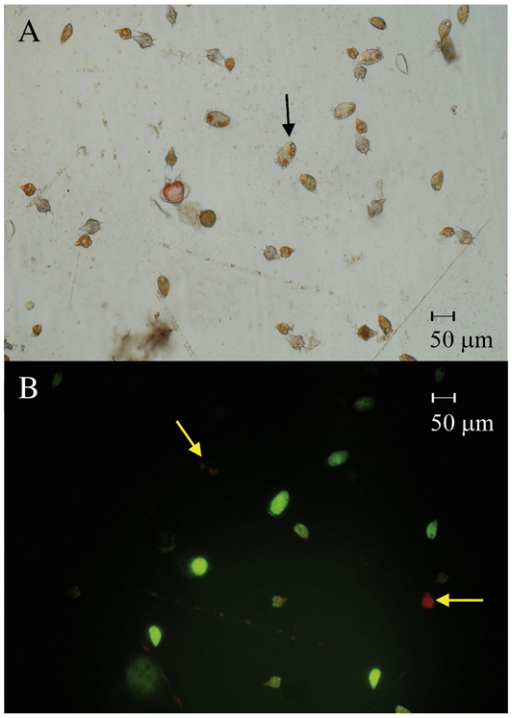

Fig. 8. An FDA-treated field sample. (A) The black arrow indicates metabolically-active cell of *D. acuminata* in DIC micrograph, and (B); yellow arrow indicate non metabolically-active cells with weak fluorescence or with no fluorescence at all.

from the CTD casts exceeded 19 °C at surface and exhibited strong horizontal and vertical gradients in the study area (Fig. 5).

Vertical distribution of *D. acuminata* in BV showed that the population was located between the surface and the upper pycnocline (1–4 m depth; Table 2, Fig. 5) within a community dominated by

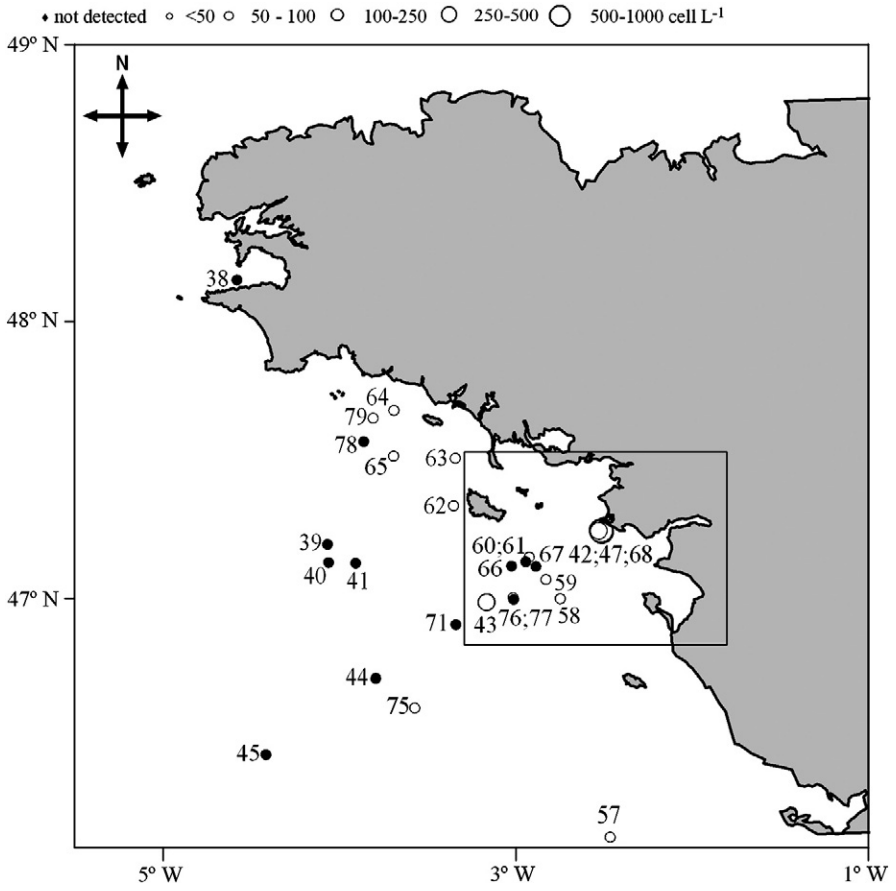

Fig. 7. Horizontal distribution of *D. acuminata* cell maxima in the Northern Bay of Biscay during the second leg of the survey (13–22 July 2006).

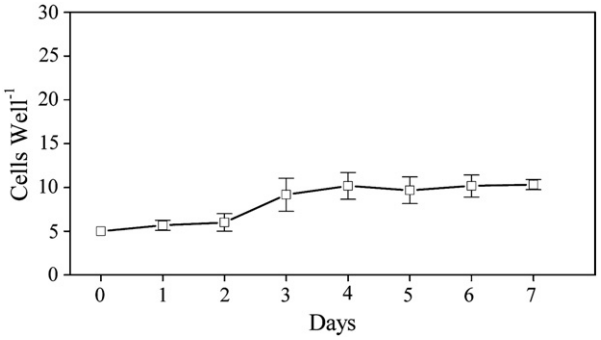

Fig. 9. Incubations (5 cells Well^{-1}) of *D. acuminata* from BV. Moderate growth: $\mu_{max} = 0.10\ d^{-1}$ was observed.

other dinoflagellates (*Prorocentrum micans*, *Ceratium fusus* and *Gonyaulax diacantha*). *D. acuminata* maxima were never found associated with the chlorophyll *a* (Chl *a*) maxima. The maximum concentration (1002 cells L^{-1}) was observed on station 31 at 2.25 m depth ($T = 18.5$ °C, $S = 33.8$, Fluorescence equivalent to 0.85 µg Chl *a* L^{-1}) on 11 July (Fig. 6). At this point, the phytoplankton community located at the Chl *a* maximum (15 m; $F = 14.5$ µg Chl *a* L^{-1}) was primarily composed of the haptophyte *Chrysochromulina* sp., that developed into a dense thin layer during the second leg of the cruise (Farrell, 2010). The diatom assemblage was dominated by a mixture of *Leptocylindrus danicus*, *L. minimus* and medium-sized *Chaetoceros* spp. and a dinoflagellate assemblage dominated by *Prorocentrum* spp. and ecdysal cysts of *Fragilidium subglobosum.*

The horizontal distribution of *D. acuminata* during the second leg of the cruise (13–22 July) (Fig. 7) showed that, unlike during the first leg, concentrations of *D. acuminata* during this period were very low (<100 cells L^{-1}) in the whole study area.

3.3. Physiological conditions of D. acuminata

No parasites were seen in any of the live samples observed by epifluorescence.

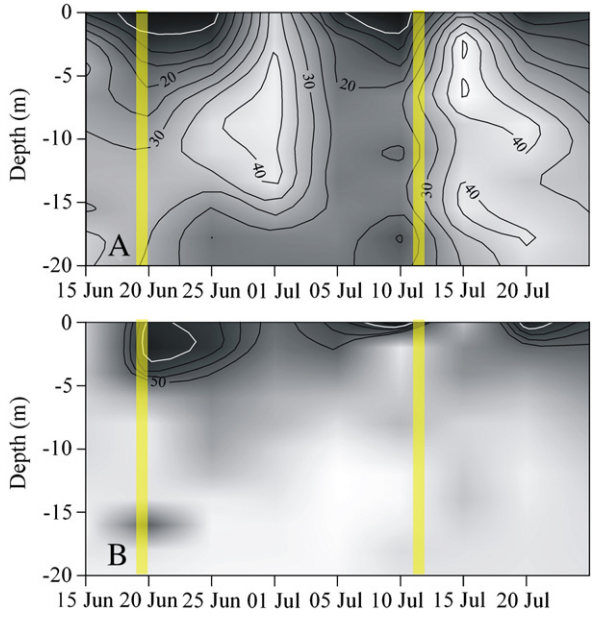

Fig. 10. Percentages of retained particles obtained from Ichthyop runs in the BV from 15 June to 30 July 2006 in (A) Area 1 (sta 31) and (B) Area 2. Vertical bars mark when *D. acuminata* reached its maximum concentration (data on 19 June from REPHY and on 11 July from cruise) in the BV. White isolines represent 5% and 35% of retention in A and B respectively.

Most *D. acuminata* cells in FDA-treated samples appeared to be in good condition, with branched, brightly autofluorescent (orange) chloroplasts. The fraction of viable cells was higher than 89% in all samples analyzed (Table 2). Therefore, a predominance of green-fluorescing metabolically-active cells was observed although some non metabolically-active cells with weak red or with no fluorescence at all were also found (Fig. 8).

Individually picked cells of *D. acuminata* incubated in the well-plates showed moderate growth (max. 0.10 d^{-1}). At the beginning of the experiment, *D. acuminata* cell numbers increased, but they stopped dividing from day 4 onwards (Fig. 9).

3.4. Modelling simulations

Results from the first set of Ichthyop model simulations showed that, on average, particle retention in Area 1(Fig. 10A) and Area 2 (Fig. 10B) increased with depth. The estimated retention in Area 1 was highest from 25 June to 5 July and from 12 to 20 July. Minimum values of retention were at 0–5 m depth on 20–23 June and 10 July (<10% retention). Although the minimum-retention periods in the whole BV region (Area 2; Fig. 10B) coincided with those in Area 1 (0–5 m), the proportion of retained particles in Area 2 (35%) was much higher than in the estimates for Area 1 (5%).

The second set of Ichthyop model simulations was used to study the retention–dispersion pattern of the *D. acuminata* maximum found during the cruise at station 31 (2–5 m depth; Fig. 11). Retention decreased from 95% on 10 July to 27% on 13–14 July in Area 1. The analysis of particle trajectories revealed that, on 9–10 July, most of the particles were still found in Area 1 (Fig. 11). The general southward transport obtained on 11–14 July was in agreement with velocity field estimated by MARS3D (Fig. 12). Simulations from MARS3D showed the establishment of an eddy offshore of the estuaries (Fig. 12). Later, on 15–18 July (Fig. 11E, F), the patch became less evident and spread offshore and northwards. At the end of the simulation, only 7% of the particles were retained in Area 1. However, as in the first set of simulations, most particles remained, though dispersed, in Area 2 by the end of the experiment.

4. Discussion

The growing season of *D. acuminata*—defined in previous studies to occur from April to September in the BV (Xie et al., 2007)—started by the end of April in 2006, but finished unusually early, by the end of July, i.e. 1 month after reaching its seasonal cell maximum (19 June). Although high concentrations (>10^3 cell L^{-1}) of *Dinophysis* spp. were not found during the cruise, substantial information was gathered on the physiological status of *D. acuminata* and on the conditions associated with the bloom decline.

4.1. Effect of biological processes during the decline of the bloom

Several biological processes, such as mortality, arrested division, encystment and parasitism, have been identified as key processes in the decline of some dinoflagellate blooms (Zingone and Wyatt, 2004). Nevertheless, observations of various biological aspects of the *D. acuminata* population during this cruise suggest that biological factors were not likely the primary cause of the collapse of the population.

On board observations suggest that *Dinophysis* populations in the area were healthy, with a high fraction (>89%) of viable cells. Incubation experiments showed a moderate (0.1 d^{-1}) division rate for this species. No significant concentrations of potential grazers of *D. acuminata*, such as heterotrophic dinoflagellates, were detected. Parasitism has been recognized as an important control of some bloom-forming dinoflagellates (Park et al., 2004; Montagnes et al., 2008). Recently, *D. acuminata* has been reported to be one of the many hosts for endoparasitic dinoflagellates of the genus *Amoebophrya*

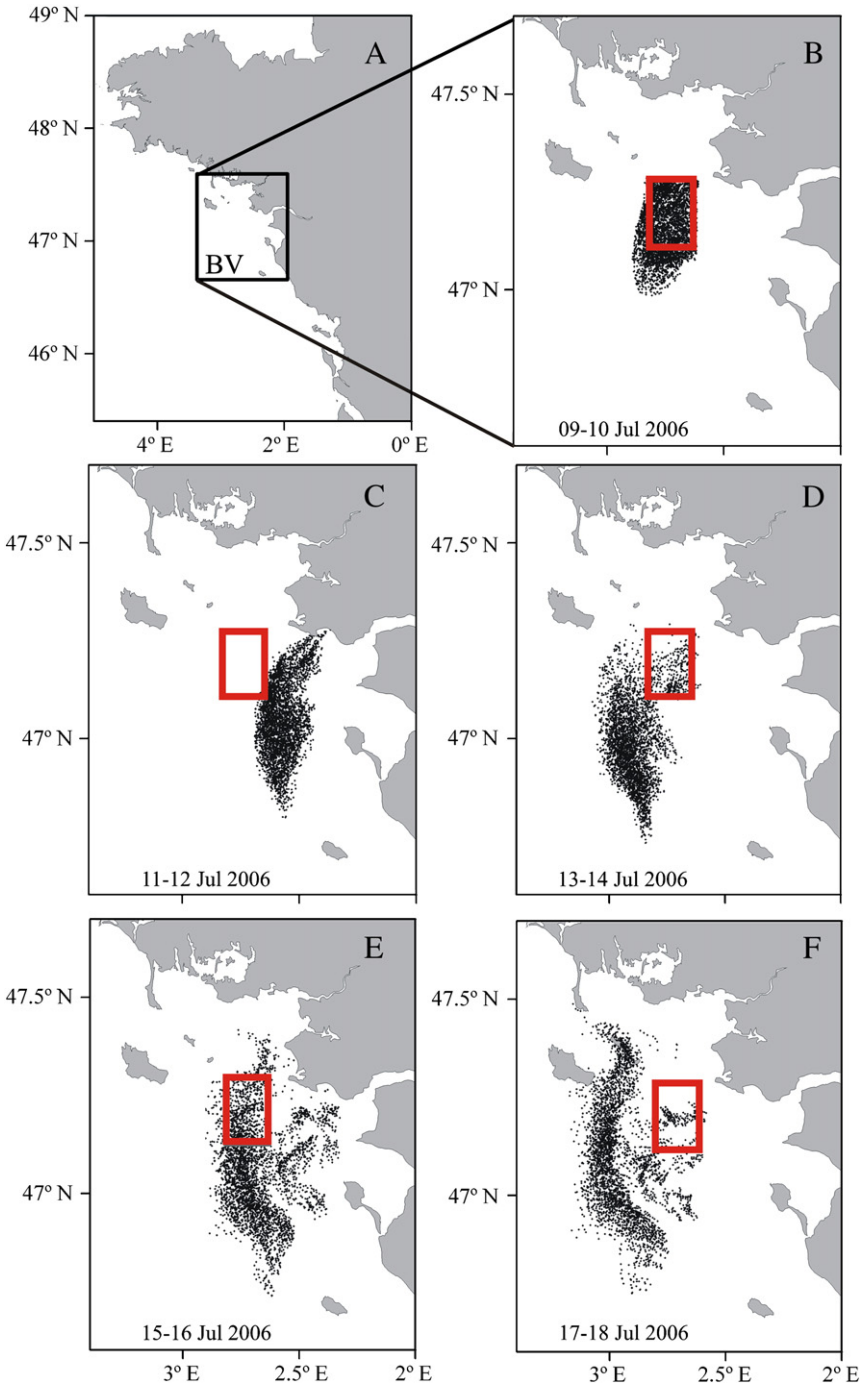

Fig. 11. Results from Ichtyop transport scenarios from 9 July to 18 July at 2–5 m depth. (A) Map of the northern Bay of Biscay showing Area 2. Position of particles after (B) 2-day, (C) 4-day, (D) 6-day, (E) 8-day, and (F) 10-day simulation are shown as black dots. Red box indicates the location of Area 1.

(Salomon et al., 2009; González-Gil et al., 2010) and for that reason, special attention was paid to detect infected *D. acuminata* cells during this survey. Frequencies of infected cells were always below detection limits, so parasitism by *Amoebophrya* was probably not a significant loss factor.

Allelopathy can also play a role in bloom decline and algal succession (Granéli et al., 2008). Among others, the allelopathic effects of *Chrysochromulina polylepis* include an initial decrease in growth rate of tested algae, followed by decline in their population numbers (Schmidt and Hansen, 2001). In our study, the decline of *D. acuminata* coincided with the onset of a *Chrysochromulina* sp. bloom that formed a conspicuous thin layer in the pycnocline during the second leg of the cruise (Farrell, 2010). Nevertheless, *D. acuminata* populations were always located near the surface (0–4 m; Table 2), well above the *Chrysochromulina* sp. cell maximum which was observed around 15 m depth in the pycnocline.

4.2. Physical processes, physical–biological interactions, and modelling results

The importance of water transport in the population dynamics of *Dinophysis* spp. and the advection of shelf populations to coastal areas has been described in several studies (i.e. Delmas et al., 1992; Belgrano et al., 1999; Escalera et al. 2010). Physical driving forces,

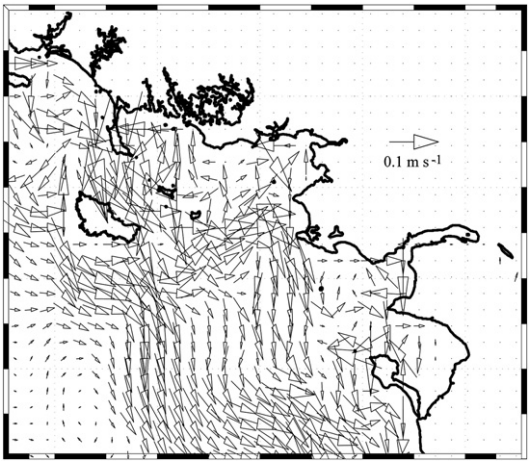

Fig. 12. Residual current field at mid depth on 13 July 2006 from MARS 3D simulations. Vectors of currents are drawn for every fourth grid node.

such as wind and/or currents that provoke accumulation–dispersion of *Dinophysis* cells have been already reported by different authors (Soudant et al., 1997; Koike et al., 2001; Koukaras and Nikolaidis, 2004). Soudant et al. (1997) explained *D. acuminata* abundance in Antifer (Normandy, France) using a dynamic linear regression. They concluded that the disappearance of *D. acuminata* cells in the area was mainly driven by northeasterly winds that provoked cell dispersion and by increased tidal forcing that induced *D. acuminata* dispersal by dilution and water-masses movement. More recently, *Dinophysis* events have been related to the onshore transport of an eddy, located offshore in the BV (Xie et al., 2007), that may constitute a retention area or "incubator" for *D. acuminata*. Xie et al. (2007) related increased densities of *Dinophysis* spp. to retentive zones where horizontal dispersion of the growing population was limited. Our results indicate that, from 9 to18 July, the *D. acuminata* population located at 2–5 m depth followed the movement of the Loire and Vilaine plumes. Particles were transported southwards but the eddy located off the Bay blocked offshore dispersion of particles until 16 July (Fig. 11, Fig. 12). Therefore, simulations from this study agree with the hypothesis of trapping of phytoplankton populations in the BV as an important factor that drives *D. acuminata* dynamics (Xie et al., 2007).

Results from the first set of Ichthyop simulations also indicate the key role of physical transport in *D. acuminata* population dynamics. Simulations of minimum particle retention coincided with the disappearance of the *D. acuminata* peaks detected on 19 June by the monitoring programme (REPHY data; Fig. 3) and on 11 July during the survey (Fig. 4). Moreover, maximum percentages of particle dispersion were found at the surface, where the *D. acuminata* cell maxima were observed (Table 2, Fig. 6) during the cruise. On the other hand, cruise observations showed that maximum concentrations of *D. acuminata* were found in Area 1 on 11 July. In Area 1, maximum particle retention given by model simulations corresponded to 12–20 July (Fig. 10). This retention pattern can explain the *D. acuminata* maxima found in the study area during the survey and its later dispersion and disappearance (Figs. 3 and 7).

Several studies in the BV have reported concentrated populations of *D. acuminata* located around marked temperature and salinity gradients (Gentien et al., 1995; Maestrini, 1998; Marcaillou et al., 2001; Lunven et al., 2005). In contrast, results from this survey showed that *D. acuminata* populations were mainly located in the upper layers. It is surprising that the *D. acuminata* cell maximum was located in the top 5 m, where a temperature anomaly of 2.98 °C (relative to the previous 22-year mean value) was found, and where the maximum wind-forced dispersion was estimated by the model. The mechanisms that triggered this aggregation near the surface are unknown, but it could well represent a dispersal phase, during late stages of bloom development within the annual cycle of *D. acuminata*. Escalera et al. (2006) described a seasonal trend in the vertical distribution of *D. acuminata* in the Galician Rías (NW Spain) from early growth starting in the pycnocline, to later stages nearer the surface. These authors drew attention to high SST values as the cause for the early decline of *D. acuminata* blooms in that area. Results from this study support the hypothesis of a dispersal strategy, which might be temperature-related, at the end of the *D. acuminata* growth season.

High dilution rates promoted by sea currents can be expected to influence dinoflagellate life cycle transitions or even disperse them completely (Zingone and Wyatt, 2004). Results from Ichthyop show that although *D. acuminata* may have been dispersed from its bloom location (Area 1), approximately 35% of the population remained in the BV during the study period (Area 2; Fig. 10). Those cells still present in the area were in good physiological condition, and may have acted as the seed for the next *D. acuminata* peak, detected after the cruise by REPHY (Fig. 3), followed by the disappearance of *D. acuminata* at the beginning of August 2006.

5. Conclusions

The application of a 3D LPTM to the population dynamics of a HAB species shows how such a model is able to reproduce *D. acuminata* patches and dispersion patterns observed in the field. Comparisons between survey data (*D. acuminata* concentrations) and model output (% of virtual particle retention) were in good agreement (Fig. 4, Fig. 7 and Fig. 10), despite the simplifications used in the model (i.e. passive particle movement). Model simulations together with biological observations suggest that, in this case, physical factors (wind-generated turbulence, advection, etc.) were a primary cause of the rapid collapse of a HAB population. This study underscores the importance of physical processes as a mechanism controlling the decline of *D. acuminata* blooms in the BV and provides confidence to set up, in the near future, a 3D LPTM of the population dynamics of *D. acuminata* for this region.

Acknowledgments

We thank the crew of *R/V Thalassa* for their help, M.M. Daniélou, E. Le Gall, A. Youenou and I. Ramilo for technical assistance. This work was funded by projects HABIT (EC 6FP, GOCE-CT-2005-003932) and TURDIRRIAS (CTM2006-13884-CO2-02/MAR). This is a contribution to the GEOHAB Core Research Project HABs and Stratification.

References

Aminot, A., Kerouel, R., 2004. Hydrologie des écosystèmes marins. Paramètres et analyses. Collection Méthodes d'analyse en milieu marin. IFREMER, France.
Belgrano, A., Lindahl, O., Hernroth, B., 1999. North Atlantic Oscillation, primary productivity and toxic phytoplankton in the Gullmar Fjord, Sweden (1985–1996). Proc. Roy. Soc. Lond. B. Biol. 266, 425–430.
Delmas, D., Herbland, A., Maestrini, S.Y., 1992. Environmental conditions which lead to increase in cell density of the toxic dinoflagellates *Dinophysis* spp. in nutrient-rich and nutrient-poor waters of French Atlantic coast. Mar. Ecol. Prog. Ser. 89, 53–61.
Delmas, D., Herbland, A., Maestrini, S.Y., 1993. Do *Dinophysis* spp. come from the "open sea" along the French Atlantic coast? In: Smayda, T., Shimizu, Y. (Eds.), Toxic Phytoplankton Blooms in the Sea. Elsevier, Amsterdam, pp. 489–494.
Dodson, A.N., Thomas, W.H., 1978. Reverse filtration. In: Sournia, A. (Ed.), Phytoplankton Manual. UNESCO, Paris, pp. 104–106.
Escalera, L., Reguera, B., Pazos, Y., Moroño, A., Cabanas, J.M., 2006. Are different species of *Dinophysis* selected by climatological conditions? Afr. J. Mar. Sci. 28, 283–288.
Escalera, L., Reguera, B., Moita, T., Pazos, Y., Cerejo, M., Cabanas, J.M., Ruiz-Villarreal, M., 2010. Bloom dynamics of *Dinophysis acuta* in an upwelling system: *in situ* growth *versus* transport. Harmful Algae 9, 312–322.
Farrell, H., 2010. Sub surface thin layers: the influence of physical processes on phytoplankton distributions in stratified marine systems. Ph.D Thesis, National University of Ireland, Galway, 332 pp.
Gallego, A., North, E.W., Petitgas, P., 2007. Introduction: status and future of modelling physical–biological interactions during the early life of fishes. Mar. Ecol. Prog. Ser. 347, 122–126.

Gentien, P., 1986. A method for evaluating phytoplankton viability by induced fluorochromasia. In: Manzoli, F.A. (Ed.), Progress in Flow Cytometry. ISBN: 90-9001361-X, pp. 151–164.
Gentien, P., Lunven, M., Lehatre, M., Dunvent, J.L., 1995. *In situ* depth profiling of particles sizes. Deep Sea Res. I 42, 1297–1312.
González-Gil, S., Velo-Suárez, L., Gentien, P., Ramilo, I., Reguera, R., 2010. Phytoplankton assemblages and characterization of *Dinophysis acuminata* population during an upwelling–downwelling cycle. Aquat. Microb. Ecol. 58, 273–286.
Granéli, E., Salomon, P.S., Fistarol, G.O., 2008. The role of allelopathy for harmful algae bloom formation. In: Evangelista, V., Barsati, L., Frassanito, A.M., Passarelli, V., Gualtieri, P. (Eds.), Algal Toxins: Nature, Occurrence, Effect and Detection. NATO Science for Peace and Security Series A: Chemistry and Biology. Springer, Netherlands, pp. 159–178.
Koike, K., Otobe, H., Takagi, M., Yoshida, T., Ogata, T., Ishimaru, T., 2001. Recent occurrences of *Dinophysis fortii* (dinophyceae) in the Okkirai Bay, Sanriku, Northern Japan, and related environmental factors. J. Oceanogr. 57, 165–175.
Koukaras, K., Nikolaidis, G., 2004. *Dinophysis* blooms in the Greek coastal waters (Thermaikos Gulf, NW Aegean Sea). J. Plankton Res. 26, 445–457.
Lazure, P., Dumas, F., 2008. An external–internal mode coupling for a 3D hydrodynamical model at regional scale (MARS). Adv. Wat. Res. 31, 233–250.
Lazure, P., Jegou, A.M., 1998. 3D modelling of seasonal evolution of Loire and Gironde plumes on Biscay Bay continental shelf. Oceanol. Acta 21, 165–177.
Lazure, P., Dumas, F., Vrignaud, C., 2008. Circulation on the Armorican shelf (Bay of Biscay) in autumn. J. Mar. Syst. 72, 218–237.
Lett, C., Verley, P., Mullon, C., Parada, C., Brochier, T., Penven, P., Blanke, B., 2008. A Lagrangian tool for modelling ichthyoplankton dynamics. Environ. Modell. Softw. 23, 1210–1214.
Lunven, M., Guillaud, J.F., Youenou, A., Crassous, M.P., Berric, R., Le Gall, E., Kerouel, R., Labry, C., Aminot, A., 2005. Nutrient and phytoplankton distribution in the Loire River plume (Bay of Biscay, France) resolved by a new Fine Scale Sampler. Estuar. Coast. Shelf Sci. 65, 94–108.
Maestrini, S.Y., 1998. Bloom dynamics and ecophysiology of *Dinophysis* spp. In: Anderson, D.M., Cembella, A.D., Hallegraeff, G.M. (Eds.), Physiological Ecology of Harmful Algae Blooms: Vol. NATO ASI, Series G of Ecological Sciences, vol. 41. Springer, Berlin Heidelberg, New York, pp. 243–266.
Maestrini, S.Y., Berland, B.R., Grzebyk, D., Spano, A.M., 1995. *Dinophysis* spp. cells concentrated from nature for experimental purposes, using size fractionation and reverse migration. Aquat. Microb. Ecol. 9, 177–182.
Marcaillou, C., Gentien, P., Lunven, M., Grand, J.L., Mondeguer, F., Daniélou, M.M., Crassous, M.P., Youenou, P., 2001. *Dinophysis acuminata* distribution and specific toxin content in relation to mussel contamination. In: Hallegraeff, G.M., Blackburn, S.I., Bolch, C.J., Lewis, R.J. (Eds.), Harmful Algal Blooms. IOC of UNESCO, Paris, pp. 356–359.
Montagnes, D.J.S., Chambouvet, A., Guillou, L., Fenton, A., 2008. Responsibility of microzooplankton and parasite pressure for the demise of toxic dinoflagellate blooms. Aquat. Microb. Ecol. 53, 211–225.
North, E.W., Gallego, A., Petitgas, P. (Eds.), 2009. Manual of recommended practices for modelling physical–biological interactions 580 during fish early life. In: ICES Cooperative 581 Research Report, vol. 295. 111 pp.
Park, M.G., Yih, W., Coats, D.W., 2004. Parasites and phytoplankton, with special emphasis on dinoflagellate infections. J. Eukaryot. Microbiol. 51, 146–155.
Salomon, P.S., Granéli, E., Neves, M.H.C.B., Rodríguez, E.G., 2009. Infection by *Amoebophrya* spp. parasitoids of dinoflagellates in a tropical marine coastal area. Aquat. Microb. Ecol. 55 (2), 143–153.
Santos, A.M.P., Chicharo, A., Dos Santos, A., Moita, T., Oliveira, P.B., Peliz, A., Re, P., 2007. Physical–biological interactions in the life history of small pelagic fish in the western Iberia upwelling ecosystem. Prog. Oceanogr. 74 (2–3), 192–209.
Schmidt, L.E., Hansen, P.J., 2001. Allelopathy in the prymnesiophyte *Chrysochromulina polylepis*: effect of cell concentration, growth phase and pH. Mar. Ecol. Prog. Ser. 216, 67–81.
Soudant, D., Beliaeff, B., Thomas, G., 1997. Explaining *Dinophysis* cf. *acuminata* abundance in Antifer (Normandy, France) using dynamic linear regression. Mar. Ecol. Prog. Ser. 156, 67–74.
Utermöhl, H., 1931. Neue wege in der quantitativen Erfassung des Planktons (mit besonderer Berücksichtigung des Ultraplanktons). Verh. Int. Ver. Theor. Angew. Limnol. 5, 567–596.
Velo-Suárez, L., González-Gil, S., Gentien, P., Lunven, M., Bechemin, C., Fernand, L., Raine, R., Reguera, B., 2008. Thin layers of *Pseudo-nitzschia* spp. and the fate of *Dinophysis acuminata* during an upwelling–downwelling cycle in a Galician Ría. Limnol. Oceanogr. 53, 1816–1834.
Xie, H., Lazure, P., Gentien, P., 2007. Small scale retentive structures and *Dinophysis*. J. Mar. Syst. 64, 173–188.
Zingone, A., Wyatt, T., 2004. Harmful algal blooms: keys to the understanding of phytoplankton ecology. In: Robinson, A.R., Brink, K.H. (Eds.), The Global Coastal Ocean: Multi-Scale Interdisciplinary Processes, vol. 13. Harvard University Press, pp. 867–926. The Sea.